

LA-UR-03-5634

Approved for public release;  
distribution is unlimited.

*Title:* Analysis of Hot and Cold Kritz Criticals with MCNP5 and  
Temperature-Specific Nuclear-Data Libraries

*Author(s):* Russell D. Mosteller  
Robert E. MacFarlane  
Robert C. Little  
Morgan C. White

*Submitted to:* Advances in Nuclear Fuel Management III  
Hilton Head Island, SC  
October 5-8, 2003



Los Alamos National Laboratory, an affirmative action/equal opportunity employer, is operated by the University of California for the U.S. Department of Energy under contract W-7405-ENG-36. By acceptance of this article, the publisher recognizes that the U.S. Government retains a nonexclusive, royalty-free license to publish or reproduce the published form of this contribution, or to allow others to do so, for U.S. Government purposes. Los Alamos National Laboratory requests that the publisher identify this article as work performed under the auspices of the U.S. Department of Energy. Los Alamos National Laboratory strongly supports academic freedom and a researcher's right to publish; as an institution, however, the Laboratory does not endorse the viewpoint of a publication or guarantee its technical correctness.

Form 836 (8/00)

# **ANALYSIS OF HOT AND COLD KRITZ CRITICALS WITH MCNP5™ AND TEMPERATURE-SPECIFIC NUCLEAR-DATA LIBRARIES**

**Russell D. Mosteller**

Diagnostics Applications Group (X-5)  
Applied Physics Division  
Los Alamos National Laboratory  
mosteller@lanl.gov

**Robert E. MacFarlane**

Nuclear Physics Group (T-16)  
Theoretical Division  
Los Alamos National Laboratory  
ryxm@lanl.gov

**Robert C. Little and Morgan C. White**

Diagnostics Applications Group (X-5)  
Applied Physics Division  
Los Alamos National Laboratory  
rcl@lanl.gov, morgan@lanl.gov

**Keywords:** MCNP, Kritz, critical experiments, nuclear data

## **ABSTRACT**

One of the longstanding obstacles to the use of the MCNP Monte Carlo code for reactor-physics calculations has been its requirement for nuclear data libraries at the temperature of the application of interest. Recently, an auxiliary code, named “doppler,” has been developed that uses an existing nuclear data library as the basis for generating a new library at the desired temperature. Libraries have been generated for three hot Kritz benchmarks using doppler and the existing ENDF66 and SAB2002 libraries. Results obtained from MCNP5 for these hot benchmarks and their room-temperature counterparts are presented herein.

## **1. INTRODUCTION**

One of the longstanding obstacles to the use of the MCNP5 Monte Carlo code<sup>1</sup> for reactor-physics calculations has been its requirement for nuclear data libraries at the temperature of the application of interest. In principle, cross sections at a given

---

MCNP is a trademark of the Regents of the University of California, Los Alamos National Laboratory.

temperature can be adjusted to the temperature of interest using well-established procedures — the same procedures, in fact, that were used to generate the initial cross sections at that given temperature. In practice, however, other complications arise because additional nuclear data such as thermal scattering laws, commonly denoted as  $S(\alpha,\beta)$ , are required at the temperature of interest.

Recently, an auxiliary code, named “doppler,” has been developed that uses an existing nuclear data library as the basis for generating a new library at the desired temperature. doppler overcomes the obstacles associated with thermal scattering laws and certain resonance representations by interpolating between values provided at two reference temperatures. Furthermore, doppler has simple input and is straightforward to use.

doppler was used in conjunction with the existing ENDF66 continuous-energy nuclear data library<sup>2</sup> and the SAB2002 library<sup>3</sup> of thermal scattering laws to generate nuclear data for Kritz-2 benchmarks<sup>4</sup> at elevated temperatures. MCNP5 calculations then were performed for those benchmarks both at room temperature (“cold”) and at elevated temperatures (“hot”). These calculations employed the existing ENDF66 and SAB2002 libraries for the cold benchmarks and the doppler-generated libraries for the hot benchmarks.

## 2. DESCRIPTION OF BENCHMARKS

Several experiments with light-water reactor lattices were performed at the Kritz reactor in Studsvik, Sweden, in the early 1970s. Recently, data for three experiments in the Kritz-2 series have been made publicly available,<sup>5</sup> and two-dimensional and three-dimensional benchmarks for them have been established.<sup>4</sup> Those experiments are the ones designated as Kritz-2:1, Kritz-2:13, and Kritz-2:19.

These benchmarks are particularly attractive for a number of reasons. Each of the three sets of experiments had identically configured lattices at both room temperature and an elevated temperature. Consequently, these benchmarks provide a consistent basis for the determination of the reactivity impact of changes in temperature and density. Furthermore, they include configurations both with low-enriched  $\text{UO}_2$  fuel and with mixed-oxide (MOX) fuel. In addition, they include both two-dimensional models based on the measured axial buckling and three-dimensional models based on the measured critical water height. Finally, the benchmarks include measured pin-power distributions that can be compared to calculated results.

The lattices in these experiments were rectangular arrays of fuel pins immersed in water inside a pressure tank. Criticality was achieved by adjusting both the height of the water and its soluble boron content. The hot cases were pressurized so that the water remained liquid. The lattices were not placed in the center of the pressure tank but instead were placed near the intersection of its south and west walls. Consequently, the moderator region between the edge of the lattice and the wall of the tank is considerably thinner on the south and west sides than on the north and east sides.

Fuel pins of a single design were used for both the Kritz-2:1 and Kritz-2:13 experiments. They contained UO<sub>2</sub> in which the uranium had been enriched to 1.86 wt.%, and they were clad in Zircaloy-2. At room temperature, the radius of the fuel was 0.529 cm, and the outer radius of the cladding was 0.6125 cm. Kritz-2:13 contained fewer fuel pins and had a tighter pitch than Kritz-2:1.

Only MOX fuel pins were used in Kritz-2:19. Those pins contained 1.50 wt.% PuO<sub>2</sub> and were clad in Zircaloy-2. The uranium in the pins was depleted uranium, with 0.16 wt.% <sup>235</sup>U. At room temperature, the radius of the fuel was 0.4725 cm, and the outer radius of the cladding was 0.5395 cm.

A succinct summary of these benchmarks is provided in Table 1. The axial buckling is used only for the two-dimensional benchmarks, and the critical water height is used only for the three-dimensional benchmarks. Although the water actually extends 40 cm below the fuel in the three-dimensional models, the critical height is reported relative to the bottom of the fuel pins.

**Table 1** Summary of benchmarks.

Core	Fuel Type	Array size	Cold Pitch (cm)	Temp (°C)	Soluble Boron (ppm)	Water Height (cm)	Axial Buckling (10 <sup>-4</sup> cm <sup>-2</sup> )
Kritz-2:1	UO <sub>2</sub>	44 x 44	1.485	19.7	217.9	65.28	14.75
				248.5	26.2	105.52	6.25
Kritz-2:13	UO <sub>2</sub>	40 x 40	1.635	22.1	451.9	96.17	8.01
				243.0	280.1	110.96	5.98
Kritz-2:19	MOX	25 x 24	1.800	21.1	4.8	66.56	16.37
				235.9	5.2	100.01	7.70

### 3. NUCLEAR DATA FOR HOT BENCHMARKS

As noted previously, MCNP requires nuclear data at the temperature of interest. The existing ENDF66 nuclear data library and SAB2002 library of thermal scattering laws are sufficient for the cold benchmarks but not for the hot benchmarks. Previously, it would have been necessary to generate full-blown nuclear data libraries at the temperatures of the hot Kritz benchmarks using the NJOY code.<sup>6,7</sup> However, doppler provides a much simpler alternative. Because this is the first time doppler has been used to generate cross sections for benchmarks, both alternatives were pursued in this study. The results from calculations using the two sets of nuclear data then were compared to verify that doppler produces accurate cross sections for the hot Kritz benchmarks.

#### 3.1 Description of the doppler Code

For continuous energy cross sections, doppler starts with library data for a temperature below the desired temperature and then broadens the resonance cross

sections up to the desired temperature using a kernel broadening method identical to the one in the NJOY processing that created the original data library. For tables of thermal scattering laws, doppler works with two sets of data from the data library. These sets are chosen so that their temperatures bracket the desired temperature, and doppler interpolates between them for the new cross sections and  $E',\mu$  emission events. A special interpolation method is used for the emissions to account for the probabilistic nature of the representation. If probability tables for the unresolved resonance range are present, doppler also interpolates for the desired temperature using library data for temperatures above and below the desired value. doppler creates the new customized data sets, along with a modified directory (XSDIR) file. The user then can specify these new materials, old materials, or a combination of them for use in MCNP calculations.

doppler was validated by direct comparisons of broadened cross sections with results from NJOY. For an integral test, doppler was used to generate cross sections at 600 K, and the values of  $k_{\text{eff}}$  from these cross sections were compared with those from direct NJOY data at 600 K with good results. These tests demonstrate that the doppler broadening is being done correctly. In addition, plots of  $k_{\text{eff}}$  as a function of temperature were generated for some of the Kritz-2 configurations using good Monte Carlo statistics. The interpolated values fell on smooth straight lines that also passed through the points where water scattering was directly calculated using NJOY. These comparisons demonstrate that the combination of doppler broadening and thermal kernel interpolation works properly.

### 3.2 Nuclear Data Generation with NJOY and doppler

To verify that doppler performs as intended, an MCNP data library at elevated temperature was generated directly using the proven methods in NJOY. ENDF/B-VI neutron evaluations for a total of 27 isotopes were processed at a temperature of 245 °C (518.15 K). The evaluations processed were identical to those used in the original generation of the ENDF66 library. The processing methodology was also the same as for ENDF66, with one exception, namely that fission spectra for delayed neutrons were omitted. In addition, a data set for the thermal scattering law for hydrogen in light water was generated at 500 K (226.85 °C) using the same evaluated data and processing methodology as for the corresponding thermal scattering laws in the SAB2002 library. The scattering law was generated at that temperature because a restriction in NJOY limits the temperatures at which scattering laws can be generated to those that appear in ENDF/B evaluations, and that was the closest such temperature.

doppler was used in conjunction with the ENDF66 continuous-energy nuclear data library to generate cross sections for the isotopes in the three hot benchmarks. Such libraries were generated at two separate temperatures, 235 °C for the hot Kritz-2:19 (MOX) benchmark and 245 °C for the hot Kritz-2:1 and Kritz-2:13 (UO<sub>2</sub>) benchmarks. The small differences in temperature between the library data and those benchmarks is not considered significant.

doppler also was used in conjunction with the existing SAB2002 library of thermal scattering laws to generate scattering laws for hydrogen in water at 235 °C and 245 °C. In addition, a third scattering law was generated at 227 °C to correspond to the one generated directly with NJOY.

### 3.3 Comparison of Results Based on Data from NJOY and from doppler

MCNP5 calculations were performed for the two-dimensional versions of the hot Kritz benchmarks using the doppler and NJOY libraries at 245 °C. The objective of these calculations was simply to compare the results from the two libraries, not to compare them to the benchmark results *per se*. Accordingly, two modifications were made to the calculations that used the doppler library to maintain consistency with the calculations with the NJOY library. First, because the hydrogen scattering law from NJOY was generated at 500 K, the cases with the doppler library used the hydrogen scattering law for that same temperature. Second, delayed-neutron spectra were omitted from the calculations with the doppler library so that they did not have to be added to the nuclear data generated with NJOY.

Each of the six calculations employed 550 generations with 10,000 neutron histories per generation, and the results from the first 50 generations were excluded from the statistics. Consequently, the results for all six cases are based on 5,000,000 active histories.

The results from the six calculations are presented in Table 2. The difference in  $k_{\text{eff}}$  for each of the benchmarks is within a single standard deviation. Consequently, it is clear that doppler produces nuclear data that are consistent with those generated directly with NJOY.

**Table 2** MCNP5 Results from NJOY and doppler Libraries.

Core	Library	$k_{\text{eff}}$	$\Delta k$
Kritz-2:1	NJOY	$0.9914 \pm 0.0003$	—
	doppler	$0.9911 \pm 0.0003$	$-0.0003 \pm 0.0004$
Kritz-2:13	NJOY	$0.9944 \pm 0.0003$	—
	doppler	$0.9942 \pm 0.0003$	$-0.0002 \pm 0.0004$
Kritz-2:19	NJOY	$1.0005 \pm 0.0003$	—
	doppler	$1.0009 \pm 0.0003$	$0.0004 \pm 0.0004$

## 4. ANALYSIS OF BENCHMARKS

MCNP5 calculations were performed for the two- and three-dimensional versions of each of the six benchmarks. The calculations for the cold benchmarks employed nuclear data taken directly from the ENDF66 and SAB2002 libraries, while those for the hot benchmarks employed nuclear data generated by doppler. Each of the calculations employed 550 generations with 10,000 neutron histories per generation, and the results from the first 50 generations were excluded from the statistics. Consequently, the results for each of the twelve cases are based on 5,000,000 active histories.

The results obtained were compared to the benchmark values for  $k_{\text{eff}}$  and to the measured pin-by-pin fission distributions. The latter comparisons are discussed in Appendix A.

### 4.1 Kritz-2:1 Benchmarks

The values obtained for  $k_{\text{eff}}$  for the Kritz-2:1 benchmarks are presented in Table 3. While the value from the two-dimensional model of the cold benchmark is in good agreement with the benchmark value, the others are substantially lower than the benchmark value. Furthermore, there is a noticeable reactivity swing between the corresponding hot and cold models. The reactivity swing between the hot and cold three-dimensional models is consistent with that reported by other analysts (in particular, see Fig. 3 of Ref. 4). However, the hot-to-cold swing for the two-dimensional models is much larger.

After a thorough and careful review of the models found no discrepancy between the MCNP5 models and the benchmark specifications, a sensitivity study was undertaken. The most likely causes for the reactivity discrepancies are the axial buckling, the critical water height, and the soluble boron content. The reported uncertainties<sup>5</sup> for these parameters are  $\pm 2\%$  in the axial buckling,  $\pm 0.01$  cm for the water height at cold conditions,  $\pm 0.1$  to  $\pm 0.2$  cm in water height at hot conditions,  $\pm 1\%$  in the soluble boron concentration above 100 ppm, and  $\pm 1.5\%$  in the soluble boron concentration below 100 ppm.

**Table 3** MCNP5 Results for Kritz-2:1 Benchmarks.

Temperature (°C)	Dimensions	Benchmark $k_{\text{eff}}$	Library	$k_{\text{eff}}$
19.7	2	$1.0000 \pm 0.0008$	ENDF66	$0.9992 \pm 0.0003$
	3	$1.0000 \pm 0.0008$	ENDF66	$0.9900 \pm 0.0003$
248.5	2	$1.0000 \pm 0.0008$	doppler	$0.9911 \pm 0.0003$
	3	$1.0000 \pm 0.0008$	doppler	$0.9878 \pm 0.0003$

MCNP5 calculations were performed that varied the critical water height in the three-dimensional models and the axial buckling in the two-dimensional models. These changes were intentionally chosen to be greater than the stated uncertainties to ensure that statistically meaningful results were obtained, and those results then were scaled in proportion to the experimental uncertainty.

The results from the sensitivity study are presented in Table 4. The impact of the uncertainty in the water height is negligible, and the impact of the uncertainty in the axial buckling is quite small. Clearly, these uncertainties do not explain the much larger discrepancy between the benchmark and calculated values for  $k_{eff}$ . However, the uncertainty in  $k_{eff}$  associated with the uncertainty in the axial buckling is comparable to the stated uncertainty in the benchmark value. This result suggests that the uncertainty in the benchmark value for  $k_{eff}$  should be increased slightly for the two-dimensional models.

The uncertainty in the soluble boron content is only  $\pm 2$  ppm for the cold benchmark and is less than  $\pm 1$  ppm for the hot benchmark. Furthermore, the largest uncertainty in the soluble boron content for any of the six benchmarks is less than  $\pm 5$  ppm. Such small changes clearly have a negligible impact on reactivity. Consequently, no calculations for variations in the soluble boron content were performed.

**Table 4** Sensitivity Studies for Kritz-2:1 Benchmarks.

Parameter	Temp (°C)	Change	$\Delta k$	Experimental Uncertainty	Associated $\Delta k$
Axial	19.7	-8.5%	$0.0042 \pm 0.0004$	$\pm 2\%$	$\pm 0.0010$
Buckling	248.5	-8%	$0.0020 \pm 0.0004$	$\pm 2\%$	$\pm 0.0005$
Water	19.7	+1 cm	$0.0010 \pm 0.0004$	$\pm 0.01$ cm	negligible
Height	248.5	+1 cm	$0.0004 \pm 0.0004$	$\pm 0.2$ cm	negligible

#### 4.2 Kritz-2:13 Benchmarks

The values obtained for  $k_{eff}$  for the Kritz-2:13 benchmarks are presented in Table 5. The patterns are the same as those observed in Table 3, although the discrepancies are not as large. The value for  $k_{eff}$  obtained from the two-dimensional model for the cold case is in more or less reasonable agreement with the benchmark model, but the other values are substantially lower. Once again, the values from the three-dimensional model are significantly lower than those from their two-dimensional counterparts, and there is a negative swing in reactivity from the cold to the hot results.



**Table 5** MCNP5 Results for Kritz-2:13 Benchmarks.

Temperature (°C)	Dimensions	Benchmark $k_{\text{eff}}$	Library	$k_{\text{eff}}$
22.1	2	1.0000 ± 0.0008	ENDF66	0.9978 ± 0.0003
	3	1.0000 ± 0.0008	ENDF66	0.9949 ± 0.0003
243.0	2	1.0000 ± 0.0008	doppler	0.9948 ± 0.0003
	3	1.0000 ± 0.0008	doppler	0.9917 ± 0.0006

### 4.3 Kritz-2:19 Benchmarks

The values obtained for  $k_{\text{eff}}$  for the Kritz-2:19 benchmarks are presented in Table 6. Although the overall agreement with the benchmark values for  $k_{\text{eff}}$  is better than for the  $\text{UO}_2$  benchmarks, the same patterns can be discerned. The values from the three-dimensional models are significantly lower than those from their two-dimensional counterparts, and there is a negative swing in reactivity from the cold to the hot results.

**Table 6** MCNP5 Results for Kritz-2:19 Benchmarks.

Temperature (°C)	Dimensions	Benchmark $k_{\text{eff}}$	Library	$k_{\text{eff}}$
21.1	2	1.0000 ± 0.0008	ENDF66	1.0035 ± 0.0003
	3	1.0000 ± 0.0008	ENDF66	0.9967 ± 0.0003
235.9	2	1.0000 ± 0.0008	doppler	1.0009 ± 0.0003
	3	1.0000 ± 0.0008	doppler	0.9940 ± 0.0003

### 4.4 Assessment of Results

Overall, the reactivity results from the Kritz-2 benchmarks are disappointing. Although some of the two-dimensional models produce reasonable agreement with the benchmark values for  $k_{\text{eff}}$ , others do not. Furthermore, the three-dimensional models all produce values for  $k_{\text{eff}}$  that are substantially lower than the benchmark values, and there is no consistent correspondence between the results from the two-dimensional and three-dimensional models except that the values for  $k_{\text{eff}}$  from the latter always are lower than those from the former.

In addition, there are sizeable hot-to-cold reactivity swings in both the two-dimensional and three-dimensional models for all three configurations. These swings,

except for the two-dimensional model for Kritz-2:1, are consistently in the range between -0.002 and -0.0035  $\Delta k$ . Generally speaking, the magnitude of these swings is consistent with those seen by other analysts. However, this very consistency, over a variety of codes and nuclear data libraries, suggests a deficiency in the benchmark specifications.

The pin-wise fission distributions for these benchmarks are discussed in Appendix A and show generally good agreement with the measured results. However, because each benchmark contains an array of identical pins on a uniform grid, the calculated fission distributions are less sensitive to the specific conditions of the benchmark than are the calculated values for  $k_{\text{eff}}$ .

## 5. CONCLUSIONS

The results obtained from this study are both encouraging and disappointing. Comparisons of results based on the NJOY and doppler libraries clearly demonstrate that doppler produces nuclear data that are consistent with those generated directly with NJOY. On the other hand, most of the calculated values for  $k_{\text{eff}}$  are significantly lower than the benchmark values. This result is particularly disappointing, given the consistently good agreement with other lattices of UO<sub>2</sub> fuel pins.<sup>8</sup>

Two-dimensional models of the three hot benchmarks using libraries generated by doppler and by NJOY produce statistically indistinguishable results for  $k_{\text{eff}}$ . This agreement is particularly striking because the standard deviations are so small ( $\pm 0.0004 \Delta k$ ), and it clearly demonstrates that doppler produces nuclear data that are consistent with those generated directly with NJOY.

However, differences between the calculated and benchmark values for  $k_{\text{eff}}$  are widespread and substantial, ranging from 0.0035 to -0.0122  $\Delta k$ . Furthermore, there are very few consistent patterns. The three-dimensional models always produce values for  $k_{\text{eff}}$  that are not only lower than the corresponding benchmark value but also the value from the corresponding two-dimensional model. In addition, all of the models predict significant hot-to-cold reactivity swings, a pattern that has been observed by other analysts.

These results suggest that the benchmark specifications for the Kritz-2 cases may need to be revisited, at least in terms of the uncertainties assigned to the benchmark values for  $k_{\text{eff}}$ . Even apart from the hot-to-cold reactivity swings, the sensitivity studies conducted herein for the Kritz-2:1 benchmark clearly indicate that the uncertainty in the axial buckling has a significantly larger impact on reactivity than does the uncertainty in the critical water height. Consequently, at the very least, similar sensitivity studies should be conducted for the Kritz-2:13 and Kritz-2:19 benchmarks, and the stated uncertainties for the two-dimensional models should be increased relative to those for the corresponding three-dimensional models.

## ACKNOWLEDGMENTS

This research was performed at Los Alamos National Laboratory under the auspices of contract W-7405-ENG-36 with the U. S. Department of Energy.

## REFERENCES

1. X-5 MONTE CARLO TEAM, "MCNP — A General Monte Carlo N-Particle Transport Code, Version 5, Volume I: Overview and Theory," Los Alamos National Laboratory report LA-UR-03-1987 (April 2003).
2. J. M. CAMPBELL, S. C. FRANKLE, and R. C. LITTLE, "ENDF66: A Continuous-Energy Neutron Data Library for MCNP4C," *Proc. 12<sup>th</sup> Biennial Topl. Mtg. Radiation Protection and Shielding Div.*, Santa Fe, New Mexico, April 14-18, 2002, p. 19, American Nuclear Society (2002).
3. R. C. LITTLE and R. E. MACFARLANE, "SAB2002 — An S( $\alpha,\beta$ ) Library for MCNP," Los Alamos National Laboratory memorandum X-5-03-21(U), February 3, 2003.
4. I. REMEC, J. C. GEHIN, P. D'HONDT, and E. SARTORI, "OECD/NEA Kritz-2 UO<sub>2</sub> and MOX Benchmarks," *Proc. Int. Conf. New Frontiers Nucl. Tech.: Reactor Physics, Safety, and High-Performance Computing (PHYSOR 2002)*, Seoul, Korea, October 7-10, 2002, American Nuclear Society (2002).
5. E. JOHANSSON, "Data and Results for Kritz Experiments on Regular H<sub>2</sub>O/Fuel Pin Lattices at Temperatures up to 245 °C," Studsvik/NS-90/133, ISBN 91-7010-143-4, Studsvik AB, Sweden (November 1990).
6. R. E. MACFARLANE and D. W. MUIR, "The NJOY Nuclear Data Processing System, Version 91" Los Alamos National Laboratory report LA-12740-M (1994).
7. R. E. MACFARLANE, "NJOY 99/2001: New Capabilities in Data Processing," *Proc. 12<sup>th</sup> Biennial Topl. Mtg. Radiation Protection and Shielding Div.*, Santa Fe, New Mexico, April 14-18, 2002, p. 161, American Nuclear Society (2002).
8. R. D. MOSTELLER, "ENDF/B-V and ENDF/B-VI Results for UO<sub>2</sub> Lattice Benchmarks Using MCNP," *Proc. Int. Conf. Physics Nucl. Sci. Tech. (PHYSOR 98)*, Hauppauge, New York, October 1998, Vol. 2, p. 1282, American Nuclear Society (1998).

## APPENDIX A

The Kritz-2 benchmark specifications<sup>4</sup> include pin-by-pin relative fission distributions for five of the six benchmarks. (Apparently, no such measurements were made on the cold Kritz-2:1 experiment.) The documentation for the experiments<sup>5</sup> states that these results were obtained from gamma scans along an 11-cm segment of each pin. Unfortunately, it does not specify the height of that 11-cm segment. Consequently, MCNP5 tallies were made for the entire length of the pin that was immersed in water.

Only selected pins were included in the gamma scans, but their locations were the same for the hot cases as for the cold cases. The locations of the selected pins are indicated in Figure A-1. Although uncertainties associated with the measurements for individual pins have not been reported, the documentation for the experiments states that the overall standard deviation is less than 1%. However, it notes that “for some [pins] the error could be much larger than 1%, not only due to statistics but for instance due to bent [pins] or inhomogeneities of the material.”

The measured fission rates were normalized to the highest value. The MCNP5 results were normalized in a slightly different but entirely consistent fashion. Specifically, they were normalized so that the total fission rate (i.e., over all the selected pins) is the same as that for the measurements.

### A.1 Hot Kritz-2:1 Benchmark

As indicated in Fig. A-1, most of the pins selected for measurement as part of the hot Kritz-2:1 benchmark are either along the northwest-to-southeast diagonal or along a straight line that runs from the middle of the west edge of the lattice to its center. One pin near the southwest corner and one near the northeast corner also were selected. The

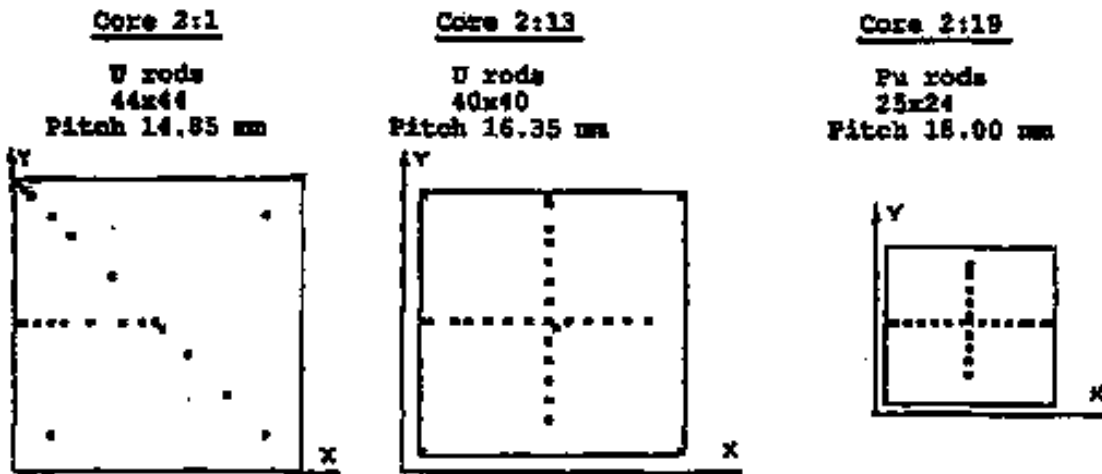


Fig. A-1 Location of selected pins in Kritz-2 Benchmarks.

results from the two- and three-dimensional models for the hot Kritz-2:1 benchmark are compared with the measured values in Table A-1.

**Table A-1** Relative fission rates for Kritz-2:1, Hot (248.5 °C).

Position*		Measured	MCNP5	
X	Y		2-D	3-D
1	23	0.7133	0.6976 ± 0.0121	0.7306 ± 0.0125
1	44	0.4309	0.4297 ± 0.0090	0.4283 ± 0.0089
2	23	0.5899	0.5581 ± 0.0101	0.5848 ± 0.0103
2	43	0.3431	0.3272 ± 0.0071	0.3301 ± 0.0070
3	42	0.3140	0.2988 ± 0.0067	0.2962 ± 0.0064
4	23	0.5689	0.5608 ± 0.0099	0.5510 ± 0.0098
6	6	0.3763	0.3746 ± 0.0075	0.3909 ± 0.0077
6	23	0.6231	0.6067 ± 0.0104	0.6181 ± 0.0107
6	39	0.3954	0.3944 ± 0.0080	0.3844 ± 0.0077
8	23	0.7074	0.6758 ± 0.0112	0.6781 ± 0.0112
9	36	0.5653	0.5442 ± 0.0096	0.5558 ± 0.0100
12	23	0.8602	0.8388 ± 0.0132	0.8350 ± 0.0131
15	30	0.7902 <sup>†</sup>	0.8621 ± 0.0136	0.8518 ± 0.0134
17	23	0.9670	0.9850 ± 0.0150	0.9675 ± 0.0148
20	23	0.9686	1.0060 ± 0.0153	1.0103 ± 0.0152
22	23	1.0000	1.0284 ± 0.0156	1.0227 ± 0.0155
23	22	0.9965	1.0420 ± 0.0158	1.0126 ± 0.0153
27	18	0.9679	0.9557 ± 0.0147	0.9488 ± 0.0146
33	12	0.7071	0.7070 ± 0.0117	0.7104 ± 0.0117
39	6	0.3832	0.3894 ± 0.0078	0.3973 ± 0.0078
39	39	0.4025	0.4067 ± 0.0082	0.3844 ± 0.0076

\* Pin in southwest corner of core is at position 1,1

<sup>†</sup> Indicated as suspicious value in Ref. 5.

There is generally good agreement between the measured and calculated fission rates. Overall, the average statistical standard deviation for the MCNP5 tallies is 1.7% for both the two- and three-dimensional models. If an average experimental standard deviation of 1% is assumed, then the combined standard deviation is approximately 2%. The standard deviation between the measured values and the corresponding MCNP tallies is 3.9% for the two-dimensional model and 3.3% for the three-dimensional model. However, if the pin with the “suspicious” measured value is omitted, those standard deviations drop to 3.1% and 2.6%, respectively. Furthermore, if that pin is omitted, the largest difference between the measured and calculated values is 4.6% for the two-dimensional model and 4.1% for the three dimensional model. Both models tend to

overpredict the power slightly in the central pins and to underpredict it slightly in the peripheral pins.

## **A.2 Kritz-2:13 Benchmarks**

As was shown in Fig. A-1, almost all of the pins selected for measurement in the Kritz-2:13 experiments are within a cruciform shape formed by straight lines running from north to south and east to west through the middle of the lattice. The results from the two- and three-dimensional models for the cold and hot Kritz-2:13 benchmarks are compared with the measured values in Tables A-2 and A-3, respectively.

The agreement between the measured and calculated fission rates for the cold benchmark is quite good. Overall, the average statistical standard deviation for the MCNP5 tallies for the cold benchmark is 1.7% for both the two-dimensional and three-dimensional models. If an average experimental standard deviation of 1% is assumed, then the combined standard deviation is approximately 2%. For both models, the standard deviation between the measured values and the corresponding MCNP tallies is the same as the average statistical standard deviation, 1.7%. Furthermore, the largest difference between the measured and calculated values is 2.6% for the two-dimensional model and 3.6% for the three dimensional model. No tilt in the fission rate is noticeable for either model.

The agreement between the measured and calculated fission rates for the hot benchmark also is very good, although not quite as good as for the cold benchmark. Overall, the average statistical standard deviation for the MCNP5 tallies for the hot benchmark is 1.4% for both the two-dimensional and three-dimensional models. If an average experimental standard deviation of 1% is assumed, then the combined standard deviation is approximately 1.5%. The standard deviation between the measured values and the corresponding MCNP tallies is 2.2% for the two-dimensional model and 1.9% for the three-dimensional model. Furthermore, the largest difference between the measured and calculated values is 4.4% for the two-dimensional model and 3.4% for the three dimensional model. No tilt in the fission rate is noticeable for either model.

## **A.3 Kritz-2:19 Benchmarks**

As was indicated in Fig. A-1, all of the pins selected for measurement in the Kritz-2:19 experiments are within a cruciform shape formed by straight lines running from north to south and east to west through the middle of the lattice. The results from the two- and three-dimensional models for the cold and hot Kritz-2:19 benchmarks are compared with the measured values in Tables A-4 and A-5, respectively.

The agreement between the measured and calculated fission rates for the cold benchmark is very good. Overall, the average statistical standard deviation for the MCNP5 tallies for the cold benchmark is 1.2% for both the two-dimensional and three-dimensional models. If an average experimental standard deviation of 1% is assumed, then the combined standard deviation is approximately 1.6%. The standard deviation

**Table A-2** Relative fission rates for Kritz-2:13, Cold (22.1 °C).

Position*		Measured	MCNP5	
X	Y		2-D	3-D
3	3	0.1570	0.1468 ± 0.0045	0.1598 ± 0.0049
3	23	0.4167	0.4207 ± 0.0085	0.4190 ± 0.0084
3	42	0.1554	0.1626 ± 0.0049	0.1633 ± 0.0049
4	23	0.3846	0.3792 ± 0.0076	0.3635 ± 0.0073
8	23	0.5573	0.5685 ± 0.0101	0.5335 ± 0.0094
10	23	0.6646	0.6611 ± 0.0112	0.6727 ± 0.0112
13	23	0.8021	0.8062 ± 0.0129	0.8043 ± 0.0129
16	23	0.9228	0.8988 ± 0.0140	0.9129 ± 0.0141
19	23	0.9608	0.9775 ± 0.0149	0.9722 ± 0.0148
22	8	0.5653	0.5555 ± 0.0099	0.5574 ± 0.0100
22	11	0.7174	0.7161 ± 0.0119	0.7322 ± 0.0121
22	14	0.8347	0.8387 ± 0.0134	0.8248 ± 0.0130
22	17	0.9192	0.9212 ± 0.0142	0.9135 ± 0.0142
22	20	0.9859	0.9621 ± 0.0147	0.9819 ± 0.0149
22	23	0.9656	0.9830 ± 0.0150	0.9862 ± 0.0149
22	26	0.9522	0.9595 ± 0.0147	0.9493 ± 0.0145
22	29	0.8907	0.8954 ± 0.0138	0.8895 ± 0.0138
22	32	0.8129	0.8091 ± 0.0130	0.7966 ± 0.0127
22	35	0.6667	0.6656 ± 0.0112	0.6635 ± 0.0111
22	37	0.5647	0.5659 ± 0.0100	0.5590 ± 0.0100
22	41	0.3802	0.3861 ± 0.0079	0.3831 ± 0.0080
22	42	0.4032	0.4109 ± 0.0084	0.4091 ± 0.0084
23	22	1.0000	0.9759 ± 0.0148	0.9941 ± 0.0150
25	23	0.9640	0.9751 ± 0.0148	0.9628 ± 0.0146
28	23	0.9256	0.9285 ± 0.0143	0.9256 ± 0.0143
31	23	0.8196	0.8341 ± 0.0132	0.8500 ± 0.0135
34	23	0.7140	0.6985 ± 0.0115	0.7207 ± 0.0119
37	23	0.5711	0.5688 ± 0.0101	0.5681 ± 0.0101
42	3	0.1536	0.1581 ± 0.0049	0.1607 ± 0.0048
42	42	0.1547	0.1532 ± 0.0047	0.1533 ± 0.0048

\* Pin in southwest corner of core is at position 3,3

between the measured values and the corresponding MCNP tallies is 2.1% for the two-dimensional model and 1.7% for the three-dimensional model. However, if the pin with the “suspicious” measured value is omitted, those standard deviations drop to 1.3% for both models. Furthermore, if that pin is omitted, the largest difference between the

**Table A-3** Relative fission rates for Kritz-2:13, Hot (243.0 °C).

Position*		Measured	MCNP5	
X	Y		2-D	3-D
3	3	0.2601	0.2517 ± 0.0057	0.2614 ± 0.0060
3	23	0.5427	0.5285 ± 0.0088	0.5386 ± 0.0088
3	42	0.2563	0.2514 ± 0.0056	0.2632 ± 0.0057
4	23	0.4858	0.4786 ± 0.0082	0.4721 ± 0.0079
8	23	0.5929	0.5985 ± 0.0093	0.6083 ± 0.0094
10	23	0.6903	0.6908 ± 0.0103	0.6895 ± 0.0103
13	23	0.8214	0.8165 ± 0.0117	0.7931 ± 0.0114
16	23	0.8951	0.9064 ± 0.0126	0.9000 ± 0.0125
19	23	0.9519	0.9564 ± 0.0131	0.9580 ± 0.0131
22	8	0.6048	0.5844 ± 0.0093	0.5936 ± 0.0093
22	11	0.7332	0.7181 ± 0.0105	0.7257 ± 0.0106
22	14	0.8563	0.8490 ± 0.0121	0.8495 ± 0.0120
22	17	0.9145	0.9037 ± 0.0125	0.9262 ± 0.0128
22	20	0.9640	0.9681 ± 0.0132	0.9820 ± 0.0134
22	23	0.9784	0.9721 ± 0.0132	0.9769 ± 0.0133
22	26	0.9375	0.9696 ± 0.0132	0.9526 ± 0.0131
22	29	0.9085	0.9075 ± 0.0126	0.8814 ± 0.0122
22	32	0.8405	0.8035 ± 0.0115	0.8307 ± 0.0119
22	35	0.6960	0.6907 ± 0.0103	0.7098 ± 0.0106
22	37	0.5983	0.6194 ± 0.0097	0.5928 ± 0.0092
22	41	0.4763	0.4891 ± 0.0081	0.5023 ± 0.0085
22	42	0.5406	0.5668 ± 0.0094	0.5400 ± 0.0089
23	22	1.0000	0.9847 ± 0.0134	0.9695 ± 0.0132
25	23	0.9628	0.9661 ± 0.0132	0.9618 ± 0.0132
28	23	0.9177	0.9367 ± 0.0130	0.9291 ± 0.0129
31	23	0.8218	0.8491 ± 0.0120	0.8252 ± 0.0117
34	23	0.7469	0.7304 ± 0.0108	0.7401 ± 0.0110
37	23	0.5985	0.6000 ± 0.0094	0.6067 ± 0.0095
42	3	0.2555	0.2524 ± 0.0057	0.2671 ± 0.0060
42	42	0.2609	0.2695 ± 0.0059	0.2626 ± 0.0058

\* Pin in southwest corner of core is at position 3,3

measured and calculated values is 2.3% for the two-dimensional model and 2.1% for the three dimensional model. No tilt in the fission rate is noticeable for either model.



**Table A-4** Relative fission rates for Kritz-2:19, Cold (21.1 °C).

Position*		Measured	MCNP5	
X	Y		2-D	3-D
2	14	0.5571	0.5587 ± 0.0076	0.5604 ± 0.0075
3	14	0.5360	0.5191 ± 0.0072	0.5282 ± 0.0073
5	14	0.6412	0.6395 ± 0.0083	0.6392 ± 0.0084
7	14	0.7648	0.7770 ± 0.0096	0.7781 ± 0.0096
9	14	0.8688	0.8887 ± 0.0106	0.8770 ± 0.0105
11	14	0.9731	0.9630 ± 0.0112	0.9597 ± 0.0113
13	14	0.9774	0.9928 ± 0.0114	0.9982 ± 0.0115
14	6	0.7697 <sup>†</sup>	0.7064 ± 0.0089	0.7215 ± 0.0091
14	8	0.8493	0.8418 ± 0.0102	0.8608 ± 0.0104
14	10	0.9275	0.9361 ± 0.0110	0.9454 ± 0.0111
14	12	0.9772	0.9882 ± 0.0114	0.9863 ± 0.0114
14	14	1.0000	1.0081 ± 0.0117	1.0070 ± 0.0117
14	15	0.9970	0.9932 ± 0.0115	1.0046 ± 0.0117
14	17	0.9367	0.9368 ± 0.0110	0.9448 ± 0.0110
14	19	0.8522	0.8567 ± 0.0104	0.8507 ± 0.0102
14	21	0.7369	0.7422 ± 0.0094	0.7333 ± 0.0092
14	22	0.6641	0.6573 ± 0.0085	0.6596 ± 0.0085
14	23	0.5941	0.6035 ± 0.0081	0.5866 ± 0.0078
16	14	0.9591	0.9789 ± 0.0114	0.9704 ± 0.0113
18	14	0.9344	0.9207 ± 0.0109	0.9324 ± 0.0110
20	14	0.8359	0.8321 ± 0.0101	0.8309 ± 0.0101
22	14	0.7063	0.7130 ± 0.0091	0.7086 ± 0.0090
23	14	0.6406	0.6471 ± 0.0085	0.6293 ± 0.0083
25	14	0.5265	0.5271 ± 0.0073	0.5116 ± 0.0071
26	14	0.5580	0.5559 ± 0.0075	0.5591 ± 0.0076

\* Pin in southwest corner of core is at position 2,2

<sup>†</sup> Indicated as suspicious value in Ref. 5.

The agreement between the measured and calculated fission rates for the hot benchmark also is very good, although not quite as good as for the cold benchmark. Overall, the average statistical standard deviation for the MCNP5 tallies for the hot benchmark is 1.2% for both the two-dimensional and three-dimensional models. If an average experimental standard deviation of 1% is assumed, then the combined standard deviation is approximately 1.6%. The standard deviation between the measured values and the corresponding MCNP tallies is 1.9% for both the two- and three-dimensional models. Furthermore, the largest difference between the measured and calculated values is 3.8% for both models. No tilt in the fission rate is noticeable for either model.

**Table A-5** Relative fission rates for Kritz-2:19, Hot (235.9 °C).

Position*		Measured	MCNP5	
X	Y		2-D	3-D
2	14	0.6953	0.6690 ± 0.0085	0.6588 ± 0.0083
3	14	0.5985	0.5926 ± 0.0078	0.5808 ± 0.0077
5	14	0.6353	0.6544 ± 0.0084	0.6577 ± 0.0085
7	14	0.7644	0.7705 ± 0.0095	0.7622 ± 0.0094
9	14	0.8583	0.8599 ± 0.0103	0.8468 ± 0.0101
11	14	0.9297	0.9250 ± 0.0108	0.9241 ± 0.0108
13	14	0.9486	0.9501 ± 0.0110	0.9491 ± 0.0110
14	6	0.7354	0.7167 ± 0.0090	0.7237 ± 0.0090
14	8	0.8216	0.8332 ± 0.0100	0.8245 ± 0.0099
14	10	0.8917	0.9034 ± 0.0106	0.9055 ± 0.0106
14	12	0.9384	0.9543 ± 0.0111	0.9512 ± 0.0110
14	14	1.0000	0.9722 ± 0.0113	0.9618 ± 0.0112
14	15	0.9459	0.9594 ± 0.0111	0.9624 ± 0.0111
14	17	0.9230	0.9063 ± 0.0106	0.9173 ± 0.0108
14	19	0.8329	0.8212 ± 0.0099	0.8370 ± 0.0101
14	21	0.7277	0.7366 ± 0.0091	0.7394 ± 0.0092
14	22	0.6856	0.6760 ± 0.0085	0.6893 ± 0.0088
14	23	0.6435	0.6325 ± 0.0082	0.6442 ± 0.0083
16	14	0.9217	0.9566 ± 0.0111	0.9448 ± 0.0110
18	14	0.9015	0.8979 ± 0.0105	0.9000 ± 0.0106
20	14	0.8170	0.8142 ± 0.0098	0.8220 ± 0.0099
22	14	0.7045	0.7150 ± 0.0090	0.7144 ± 0.0090
23	14	0.6511	0.6632 ± 0.0085	0.6538 ± 0.0084
25	14	0.6054	0.6086 ± 0.0080	0.6023 ± 0.0078
26	14	0.6898	0.6780 ± 0.0085	0.6936 ± 0.0086

\* Pin in southwest corner of core is at position 2,2